1. PETROLOGY AND SAMPLE DESCRIPTION

The most distinctive petrographic feature of the Gerba Guracha lavas is the porphyritic texture; typified by large cm-scale zoned clinopyroxene crystals that display both sector and fine-scale (possibly oscillatory) zoning set in dark, almost glassy matrix. Glomeroporphyritic textures comprised of mm scale clinopyroxene and olivine are commonly observed. In hand specimen, Gerba Guracha lavas appear fresh, an observation confirmed by petrographic examination revealing broadly unaltered crystals and matrix. Zeolite- or carbonate-filled vesicles are evident in hand specimen but were avoided during billet preparation.

2. CALCULATIONS USED TO DETERMINE TDM MODEL AGES

We calculated the time to extraction from the depleted mantle (T_{DM}) for the Sm-Nd and Lu-Hf systems on the basis of the following equation:

$$1/\lambda * \ln[\{X-Y/(\alpha - \beta)\}+1)]$$

where:

$\lambda = 6.54 \times 10^{-12}\ y^{-1}$ (Nd system) and $1.867 \times 10^{-11}\ y^{-1}$ (Hf system)

X = the measured $^{143}Nd/^{144}Nd$ or $^{176}Hf/^{177}Hf$.

Y = $^{143}Nd/^{144}Nd$ (0.51315) or $^{176}Hf/^{177}Hf$ (0.28325) of the depleted mantle

α = the measured $^{147}Sm/^{144}Nd$ or $^{176}Lu/^{177}Hf$

β = $^{147}Sm/^{144}Nd$ (0.2135) or $^{176}Lu/^{177}Hf$ (0.0384) of the depleted mantle

Values for the depleted mantle reservoirs (DM) are from Carlson and Irving (1994) and Hawkesworth et al., (2010).

3. DATA SOURCES FOR FIGURE 2 and 3

Data for Figure 2:

Gulf of Aden (Schilling et al., 1992; Rooney et al., 2012). Gulf of Aden mid ocean ridge basalts. Data are not age corrected.

St. Helena (Gast, 1968; Oversby and Gast, 1970; Sun, 1980; Cohen and O'Nions, 1982; Chaffey et al., 1989; Graham et al., 1992; Thirlwall, 1997; Salters and White, 1998)

Turkana (Furman et al., 2006). Eocene to Miocene magmas from the Turkana depression in Kenya. Data are age corrected as presented by Furman et al., (2006)

Darfur Dome (Franz et al., 1999; Lucassen et al., 2008). Eocene to recent activity in the Darfur Dome, Sudan. Data are age corrected when presented by the author.

30 Ma HT-2 (Pik et al., 1999). Oligocene HT-2 flood basalts from the Western Ethiopian Plateau. Data are age corrected as presented by Pik et al., (1999).

Jordan xenoliths (Shaw et al., 2007). Spinel lherzolite xenoliths from the shallow Jordanian sub-continental lithospheric mantle. Data are not age corrected.

Yemen xenoliths (Baker et al., 1998). Hydrous and anhydrous xenoliths from Ataq that sample the Yemeni sub-continental lithospheric mantle. These xenoliths are those that have been metasomatized by the Afar plume. Data are not age corrected.

Arabian Plate (Bertrand et al., 2003). Late Miocene to Plio-Quaternary lavas from Yemen, Saudi Arabia, Jordan, and Syria. Data are not age corrected.

Ethiopian Rift (Furman et al., 2006; Rooney et al., 2012). Quaternary lavas from the Wonji Fault Belt and Silti Debre Zeyit Fault Zone of the Main Ethiopian Rift. Data are not age corrected.

Data for Figure 3:

Sheba Ridge (Schilling et al., 1992). Regional ambient depleted mid ocean ridge basalts from the Gulf of Aden that are east of 48^{o}E. Data are not age corrected.

Gerf Ophiolite (Zimmer et al., 1995). Age corrected to 750 Ma.

Pan African Plutons are Pan African Feldspars and whole rock results on Pan African plutons (Stacey and Stoeser, 1983; Stacey and Agar, 1985). Data is mixture of corrected and uncorrected values as reported by the authors. Also included are Pan African Galenas from the Nubian-Arabian Shield (Stacey et al., 1980; Stacey and Stoeser, 1983).

Intraplate basalts are from the African-Arabian Plate (Franz et al., 1999; Bertrand et al., 58 2003; Lucassen et al., 2008).

4. SUPPLEMENTAL FIGURES

Figure DR1. Total alkali-silica diagram after Le Maitre (2002) showing the Gerba Guracha lavas and mafic lavas from other regional suites:

30 Ma LT flood basalts (Pik et al., 1998; Pik et al., 1999; Kieffer et al., 2004)

30 Ma HT-1 flood basalts (Pik et al., 1998; Pik et al., 1999)

30 Ma HT-2 flood basalts (Pik et al., 1998; Pik et al., 1999; Beccaluva et al., 2009)

Miocene-Quaternary Djibouti (Deniel et al., 1994)

Quaternary Main Ethiopian Rift (MER) (Rooney et al., 2005; Furman et al., 2006; Rooney et al., 2007; Rooney, 2010)

Miocene Shields (Kieffer et al., 2004).

Figure DR2. Variance of major element oxides and trace elements for Gerba Guracha lavas shown against the same lava suites referenced in Figure DR1. Values of Ce/Pb of 25 ± 5 are considered asthenospheric-derived (Hofmann et al., 1986).

Figure DR3. Age corrected isotopic plots for the Gerba Guracha lavas and other regional suites. The Gerba Guracha magmas have been corrected to 24 Ma. We show variability of $^{87}Sr/^{86}Sr_{(i)}$, and $^{143}Nd/^{144}Nd_{(i)}$ against $^{206}Pb/^{204}Pb_{(i)}$. Also shown is the variance of $^{87}Sr/^{86}Sr_{(i)}$-$^{143}Nd/^{144}Nd_{(i)}$.

Data sources:

Gulf of Aden (Schilling et al., 1992; Rooney et al., 2012). Gulf of Aden mid ocean ridge basalts. Data are not age corrected.

Cameroon Line (Halliday et al., 1988; Halliday et al., 1990; Lee et al., 1994; Ballentine et al., 1997). These data are not age corrected.

St. Helena (Gast, 1968; Oversby and Gast, 1970; Sun, 1980; Cohen and O'Nions, 1982; Chaffey et al., 1989; Graham et al., 1992; Thirlwall, 1997; Salters and White, 1998)

Turkana (Furman et al., 2006). Eocene to Quaternary magmas from the Turkana depression in Kenya. Data are age corrected as presented by Furman et al., (2006)

Darfur Dome (Franz et al., 1999; Lucassen et al., 2008). Eocene to recent activity in the Darfur Dome, Sudan. Data are age corrected when presented by the author.

South Africa. Late Cretaceous to Paleogene Western Cape Melilitite province, South Africa (Janney et al., 2002). These data are age corrected as presented by Janney et al., 96 (2002).

30 Ma HT-2 (Pik et al., 1999). Oligocene HT-2 flood basalts from the Western Ethiopian Plateau. Data are age corrected as presented by Pik et al., (1999).

Jordan xenoliths (Shaw et al., 2007). Spinel lherzolite xenoliths from the shallow Jordanian sub-continental lithospheric mantle. Data are not age corrected.

Arabian Plate (Bertrand et al., 2003). Late Miocene to Plio-Quaternary lavas from Yemen, Saudi Arabia, Jordan, and Syria. Data are not age corrected.

Ethiopian Rift (Furman et al., 2006; Rooney et al., 2012). Quaternary lavas from the Wonji Fault Belt and Silti Debre Zeyit Fault Zone of the Main Ethiopian Rift. Data are not age corrected.

Figure DR4. Age corrected isotopic plots for the Gerba Guracha lavas. The Gerba Guracha magmas have been corrected to 24 Ma. We show the variance of Sr, Nd and Hf isotopes versus MgO.

Figure DR5. Age corrected isotopic plots for the Gerba Guracha lavas. The Gerba Guracha magmas have been corrected to 24 Ma. We show the variance of Pb isotopes versus MgO.

Figure DR6. Primitive mantle normalized (Sun and McDonough, 1989) trace element diagram showing the Gerba Guracha lavas.

5. SUPPLEMENTAL TABLES

Table DR1. GPS Coordinates for the Gerba Guracha samples.

Table DR2. Major element and selected trace element analysis performed by XRF. Replicates were performed 6 weeks after the initial analysis and are shown in orange. Geologic standards BHVO-1, JA-3 and W-2 run as unknowns are shown for reference.

Table DR3. Trace element analysis performed by LA-ICPMS. Geological standards JB1a, JB2, JB3, and W2 run as unknowns are shown for reference.

Table DR4. Measured isotopic results for the Gerba Guracha lavas.

SUPPLEMENTAL REFERENCES

Baker, J., Chazot, G., Menzies, M., and Thirlwall, M., 1998, Metasomatism of the shallow mantle beneath Yemen by the Afar plume - Implications for mantle plumes, flood volcanism, and intraplate volcanism: Geology, v. 26, p. 431–434.

Ballentine, C.J., Lee, D.C., and Halliday, A.N., 1997, Hafnium isotopic studies of the Cameroon line and new HIMU paradoxes: Chemical Geology, v. 139, p. 111–124.

Beccaluva, L., Bianchini, G., Natali, C., and Siena, F., 2009, Continental flood basalts and mantle plumes: a case study of the Northern Ethiopian Plateau: Journal of Petrology, v. 50, p. 1377–1403.

Bertrand, H., Chazot, G., Blichert-Toft, J., and Thoral, S., 2003, Implications of widespread high-mu volcanism on the Arabian Plate for Afar mantle plume and lithosphere composition: Chemical Geology, v. 198, p. 47–61.

Carlson, R.W., and Irving, A.J., 1994, Depletion and enrichment history of subcontinental lithospheric mantle: An Os, Sr, Nd and Pb isotopic study of ultramafic xenoliths from the northwestern Wyoming Craton: Earth and Planetary Science Letters, v. 126, p. 457–472.

Chaffey, D.J., Cliff, R.A., and Wilson, B.M., 1989, Characterization of the St Helena magma source: Geological Society of London, Special Publications, v. 42, p. 257–276.

Cohen, R.S., and O'Nions, R.K., 1982, Identification of recycled continental material in the mantle from Sr, Nd and Pb isotope investigations: Earth and Planetary Science Letters, v. 61, p. 73–84.

Deniel, C., Vidal, P., Coulon, C., and Vellutini, P.J., 1994, Temporal evolution of mantle sources during continental rifting - the volcanism of Djibouti (Afar): Journal of Geophysical Research. Solid Earth, v. 99, p. 2853–2869.

Franz, G., Steiner, G., Volker, F., Pudlo, D., and Hammerschmidt, K., 1999, Plume related alkaline magmatism in central Africa—the Meidob Hills (W Sudan): Chemical Geology, v. 157, p. 27–47.

Furman, T., Bryce, J.G., Rooney, T., Hanan, B.B., Yirgu, G., and Ayalew, D., 2006, Heads and tails: 30 million years of the Afar plume, *in* Yirgu, G., Ebinger, C., and Maguire, P., eds., The Afar Volcanic Province within the East African Rift System: Special Publication of the Geological Society, London, Volume 259, p. 95-120.

Gast, P.W., 1968, The isotopic composition of lead from St. Helena and ascension islands: Earth and Planetary Science Letters, v. 5, p. 353–359.

Graham, D.W., Humphris, S.E., Jenkins, W.J., and Kurz, M.D., 1992, Helium isotope geochemistry of some volcanic rocks from Saint Helena: Earth and Planetary Science Letters, v. 110, p. 121–131.

Halliday, A.N., Davidson, J.P., Holden, P., DeWolf, C., Lee, D.-C., and Fitton, J.G., 1990, Trace-element fractionation in plumes and the origin of HIMU mantle beneath the Cameroon line: Nature, v. 347, p. 523–528.

Halliday, A.N., Dickin, A.P., Fallick, A.E., and Fitton, J.G., 1988, Mantle Dynamics: A Nd, Sr, Pb and O Isotopic Study of the Cameroon Line Volcanic Chain: Journal of Petrology, v. 29, p. 181–211.

Hawkesworth, C.J., Dhuime, B., Pietranik, A.B., Cawood, P.A., Kemp, A.I.S., and Storey, C.D., 2010, The generation and evolution of the continental crust: Journal of the Geological Society, v. 167, p. 229–248.

Hofmann, A.W., Jochum, K.P., Seufert, M., and White, W.M., 1986, Nb and Pb in oceanic basalts - New constraints on mantle evolution: Earth and Planetary Science Letters, v. 79, p. 33–45.

Janney, P.E., Le Roex, A.P., Carlson, R.W., and Viljoen, K.S., 2002, A chemical and multi- isotope study of the Western Cape olivine melilitite province, South Africa: Implications for the sources of

kimberlites and the origin of the HIMU signature in Africa: Journal of Petrology, v. 43, p. 2339–2370.

Kieffer, B., Arndt, N., Lapierre, H., Bastien, F., Bosch, D., Pecher, A., Yirgu, G., Ayalew, D., Weis, D., Jerram, D.A., Keller, F., and Meugniot, C., 2004, Flood and shield basalts from Ethiopia: Magmas from the African superswell: Journal of Petrology, v. 45, p. 793–834.

Lee, D.-C., Halliday, A.N., Fitton, J.G., and Poli, G., 1994, Isotopic variations with distance and time in the volcanic islands of the Cameroon line: evidence for a mantle plume origin: Earth and Planetary Science Letters, v. 123, p. 119–138.

R. W. Le Maitre (ed.), 2002, Igneous Rocks: A Classification and Glossary of Terms: Cambridge, UK, Cambridge University Press, 236 p.

Lucassen, F., Franz, G., Romer, R.L., Pudlo, D., and Dulski, P., 2008, Nd, Pb, and Sr isotope composition of Late Mesozoic to Quaternary intra-plate magmatism in NE-Africa (Sudan, Egypt): high-mu signatures from the mantle lithosphere: Contributions to Mineralogy and Petrology, v. 156, p. 765–784.

Oversby, V.M., and Gast, P.W., 1970, Isotopic composition of lead from oceanic islands: Journal of Geophysical Research, v. 75, p. 2097–2114.

Pik, R., Deniel, C., Coulon, C., Yirgu, G., Hofmann, C., and Ayalew, D., 1998, The northwestern Ethiopian Plateau flood basalts. Classification and spatial distribution of magma types: Journal of Volcanology and Geothermal Research, v. 81, p. 91–111.

Pik, R., Deniel, C., Coulon, C., Yirgu, G., and Marty, B., 1999, Isotopic and trace element signatures of Ethiopian flood basalts; evidence for plume-lithosphere interactions: Geochimica et Cosmochimica Acta, v. 63, p. 2263–2279.

Rooney, T., Furman, T., Bastow, I.D., Ayalew, D., and Gezahegn, Y., 2007, Lithospheric modification during crustal extension in the Main Ethiopian Rift: Journal of Geophysical Research, B: Solid Earth and Planets, v. 112, p. B10201, doi:10.1029/2006JB004916.

Rooney, T., Furman, T., Yirgu, G., and Ayalew, D., 2005, Structure of the Ethiopian lithosphere: Xenolith evidence in the Main Ethiopian Rift: Geochimica et Cosmochimica Acta, v. 69, p. 3889–3910.

Rooney, T.O., 2010, Geochemical evidence of lithospheric thinning in the southern Main Ethiopian Rift: Lithos, v. 117, p. 33–48.

Rooney, T.O., Hanan, B.B., Graham, D.W., Furman, T., Blichert-Toft, J., and Schilling, J.-G., 2012, Upper Mantle Pollution during Afar Plume–Continental Rift Interaction: Journal of Petrology, v. 53, p. 365–389.

Salters, V.J.M., and White, W.M., 1998, Hf isotope constraints on mantle evolution: Chemical Geology, v. 145, p. 447–460.

Schilling, J.G., Kingsley, R.H., Hanan, B.B., and McCully, B.L., 1992, Nd-Sr-Pb isotopic variations along the Gulf of Aden - Evidence for Afar mantle plume continental lithosphere interaction: Journal of Geophysical Research. Solid Earth, v. 97, p. 10927–10966.

Shaw, J.E., Baker, J.A., Kent, A.J.R., Ibrahim, K.M., and Menzies, M.A., 2007, The geochemistry of the Arabian lithospheric mantle - A source for intraplate volcanism?: Journal of Petrology, v. 48, p. 1495-1512.2

Stacey, J., Doe, B., Roberts, R., Delevaux, M., and Gramlich, J., 1980, A lead isotope study of mineralization in the Saudi Arabian Shield: Contributions to Mineralogy and Petrology, v. 74, p. 175–188.

Stacey, J., and Stoeser, D., 1983, Distribution of oceanic and continental leads in the Arabian- Nubian Shield: Contributions to Mineralogy and Petrology, v. 84, p. 91–105.

Stacey, J.S., and Agar, R.A., 1985, U-Pb Isotopic evidence for the accretion of a continental microplate in the Zalm region of the Saudi Arabian Shield: Journal of the Geological Society, v. 142, p. 1189–1203.

Sun, S.-S., 1980, Lead Isotopic Study of Young Volcanic Rocks from Mid-Ocean Ridges, Ocean Islands and Island Arcs: Philosophical Transactions of the Royal Society of London. Series A, Mathematical and Physical Sciences, v. 297, p. 409–445.

Sun, S.s.-., and McDonough, W.F., 1989, Chemical and isotopic systematics of oceanic basalts: Implications for mantle composition and processes., *in* Saunders, A.D., ed., Magmatism in the ocean basins: Geological Society of London Special Publication 42, p. 313-345.

Thirlwall, M.F., 1997, Pb isotopic and elemental evidence for OIB derivation from young HIMU mantle: Chemical Geology, v. 139, p. 51–74.

Workman, R.K., and Hart, S.R., 2005, Major and trace element composition of the depleted MORB mantle (DMM): Earth and Planetary Science Letters, v. 231, p. 53–72.

Zimmer, M., Kröner, A., Jochum, K.P., Reischmann, T., and Todt, W., 1995, The Gabal Gerf complex: A precambrian N-MORB ophiolite in the Nubian Shield, NE Africa: Chemical Geology, v. 123, p. 29–51.

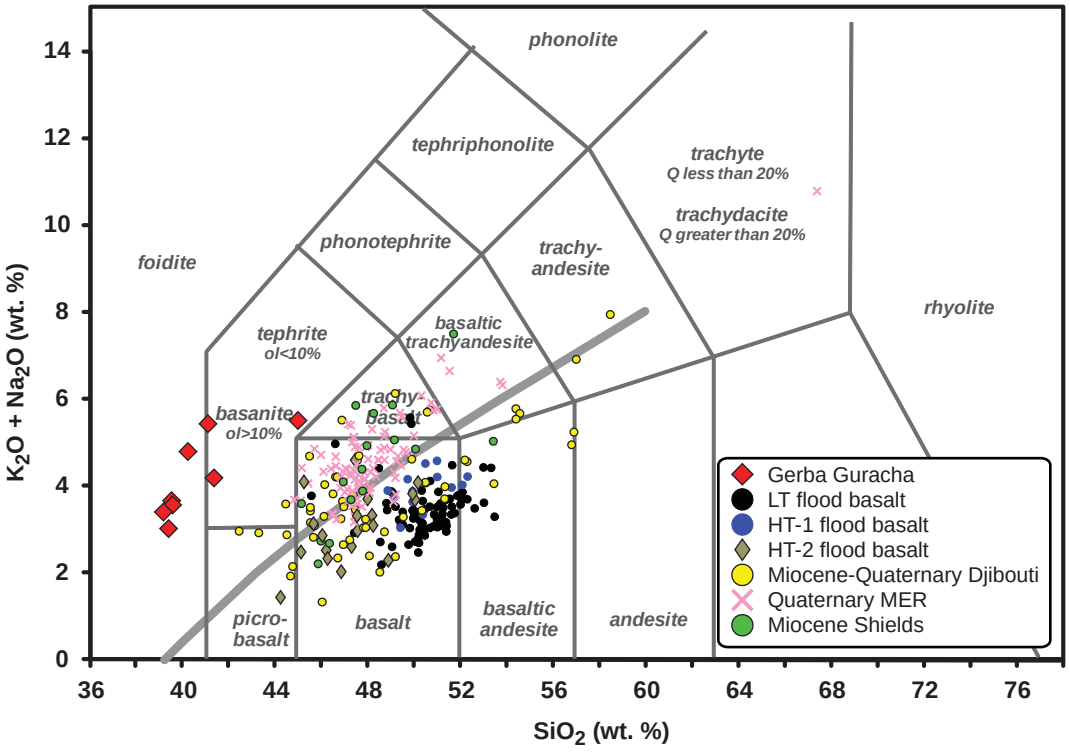
phonolite
tephriphonolite
trachyte
Q less than 20%
trachydacite
Q greater than 20%
foidite
phonotephrite
trachy-
andesite
rhyolite
tephrite
ol<10%
basaltic
trachyandesite
basanite
ol>10%
trachy-
basalt
picro-
basalt
basalt
basaltic
andesite
andesite
Gerba Guracha
LT flood basalt
HT-1 flood basalt
HT-2 flood basalt
Miocene-Quaternary Djibouti
Quaternary MER
Miocene Shields
K2O + Na2O (wt. %)
SiO2 (wt. %)
0
2
4
6
8
10
12
14
36
40
44
48
52
56
60
64
68
72
76

Figure DR1

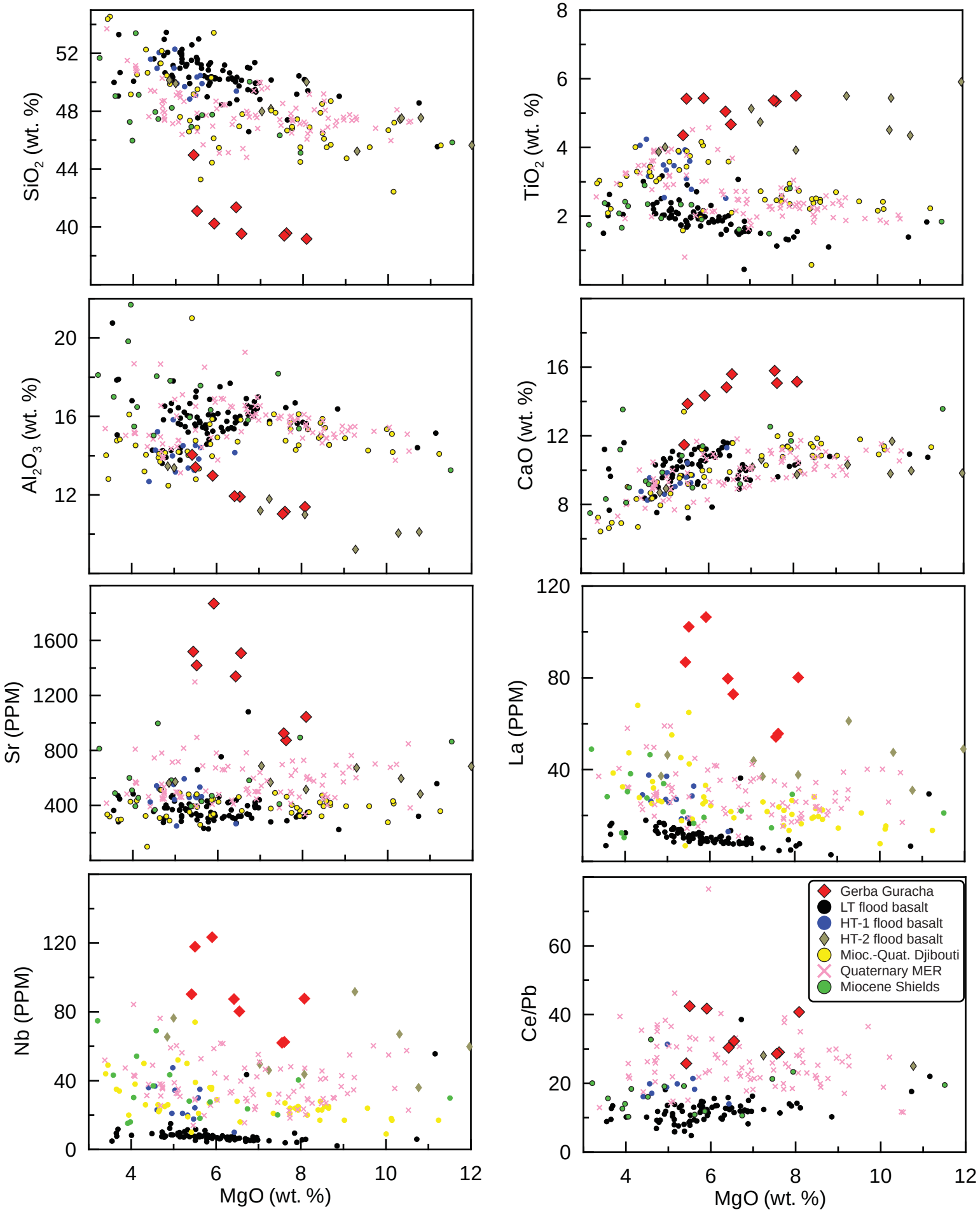
SiO2 (wt. %)
TiO2 (wt. %)
Al2O3 (wt. %)
CaO (wt. %)
Sr (PPM)
La (PPM)
Nb (PPM)
Ce/Pb
MgO (wt. %)
MgO (wt. %)
Gerba Guracha
LT flood basalt
HT-1 flood basalt
HT-2 flood basalt
Mioc.-Quat. Djibouti
Quaternary MER
Miocene Shields

Figure DR2

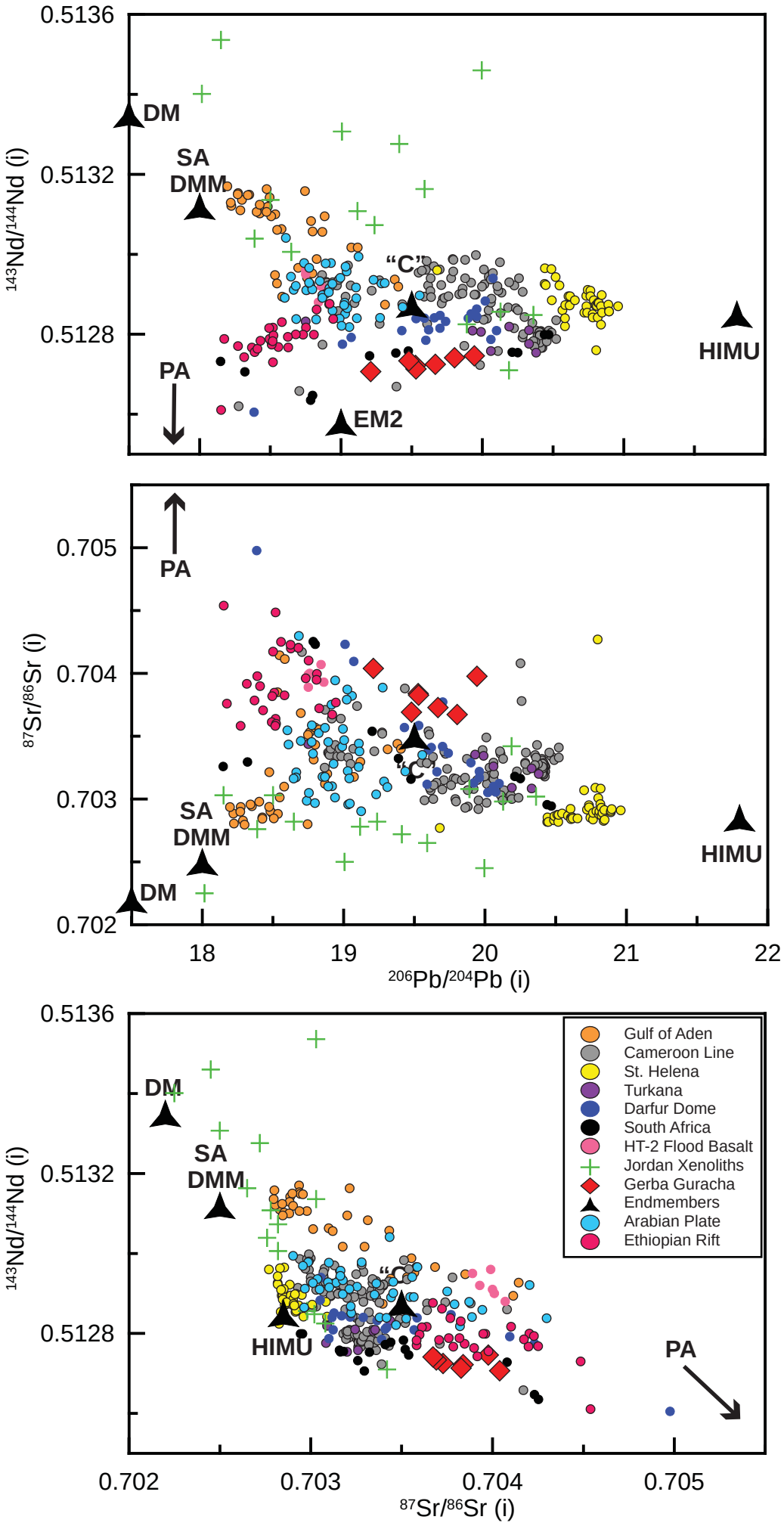
0.5136
0.5132
0.5128
143Nd/144Nd (i)
DM
SA
DMM
"C"
PA
EM2
HIMU
0.705
0.704
0.703
0.702
87Sr/86Sr (i)
18
19
20
21
22
206Pb/204Pb (i)
Gulf of Aden
Cameroon Line
St. Helena
Turkana
Darfur Dome
South Africa
HT-2 Flood Basalt
Jordan Xenoliths
Gerba Guracha
Endmembers
Arabian Plate
Ethiopian Rift

Figure DR3

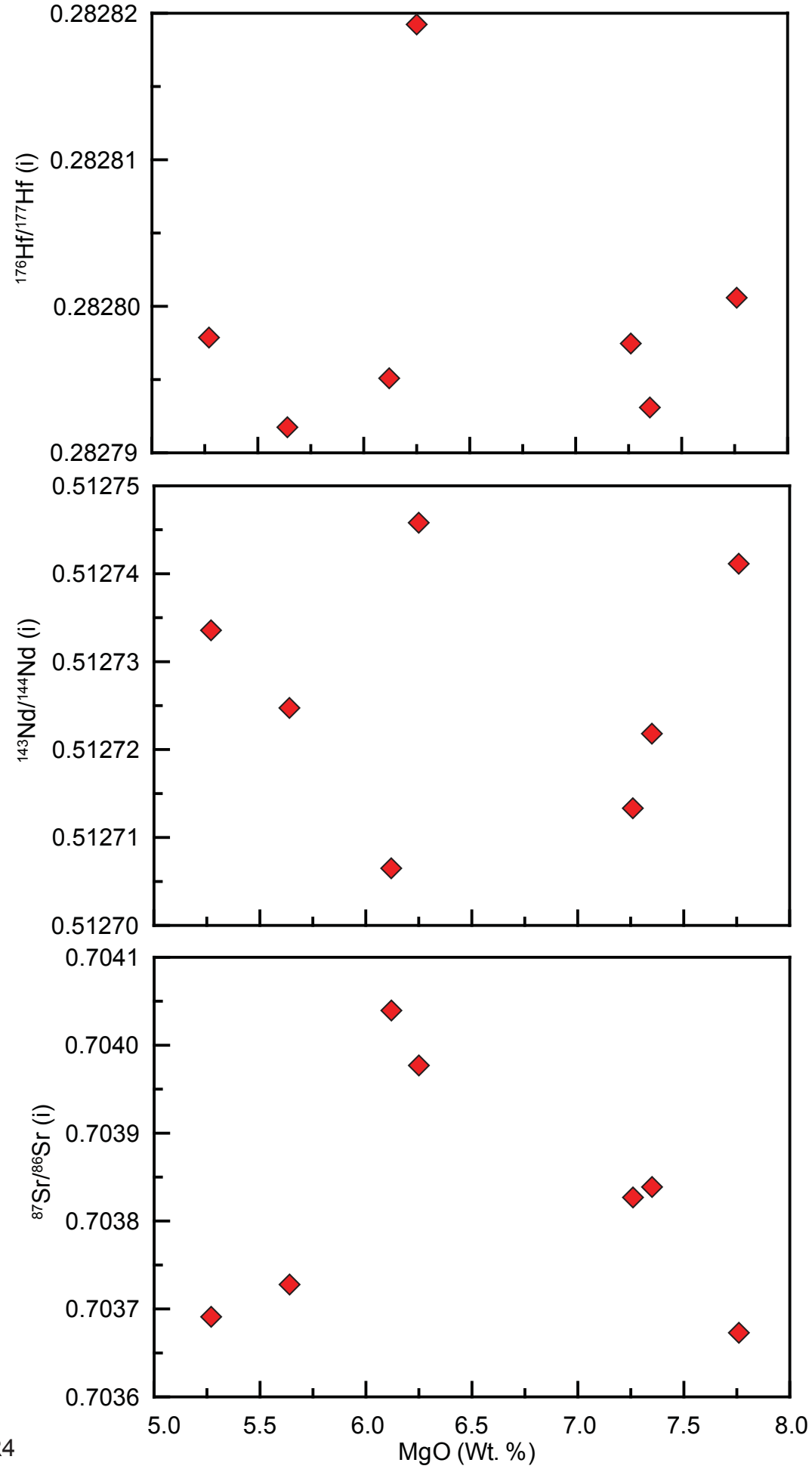
0.28282
0.28281
0.28280
0.28279
176Hf/177Hf (i)
0.51275
0.51274
0.51273
0.51272
0.51271
0.51270
143Nd/144Nd (i)
0.7041
0.7040
0.7039
0.7038
0.7037
0.7036
87Sr/86Sr (i)
5.0
5.5
6.0
6.5
7.0
7.5
8.0
MgO (Wt. %)

Figure DR4

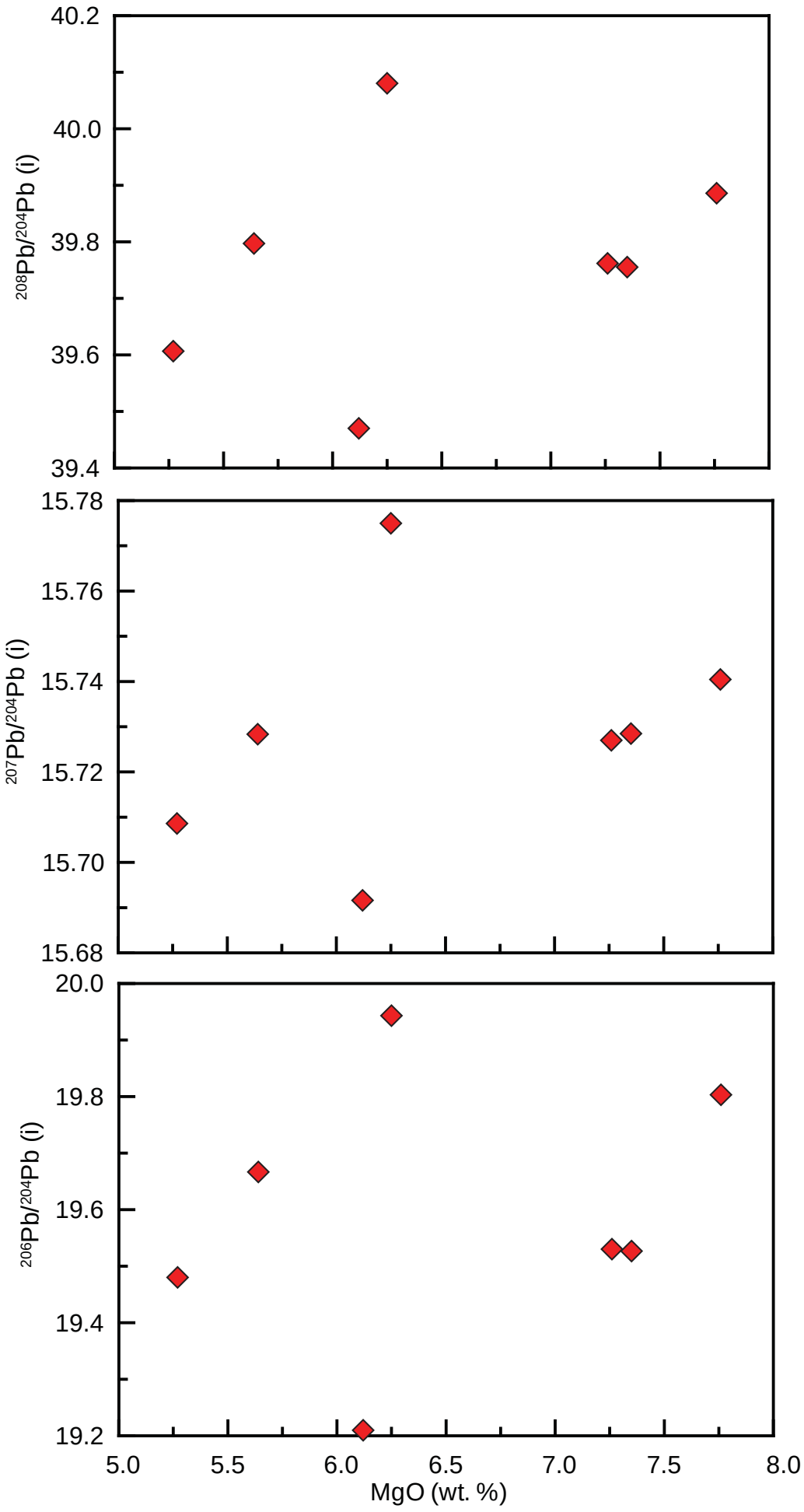
40.2
40.0
39.8
39.6
39.4
$^{208}Pb/^{204}Pb$ (i)
15.78
15.76
15.74
15.72
15.70
15.68
$^{207}Pb/^{204}Pb$ (i)
20.0
19.8
19.6
19.4
19.2
$^{206}Pb/^{204}Pb$ (i)
5.0
5.5
6.0
6.5
7.0
7.5
8.0
MgO (wt. %)

Figure DR5

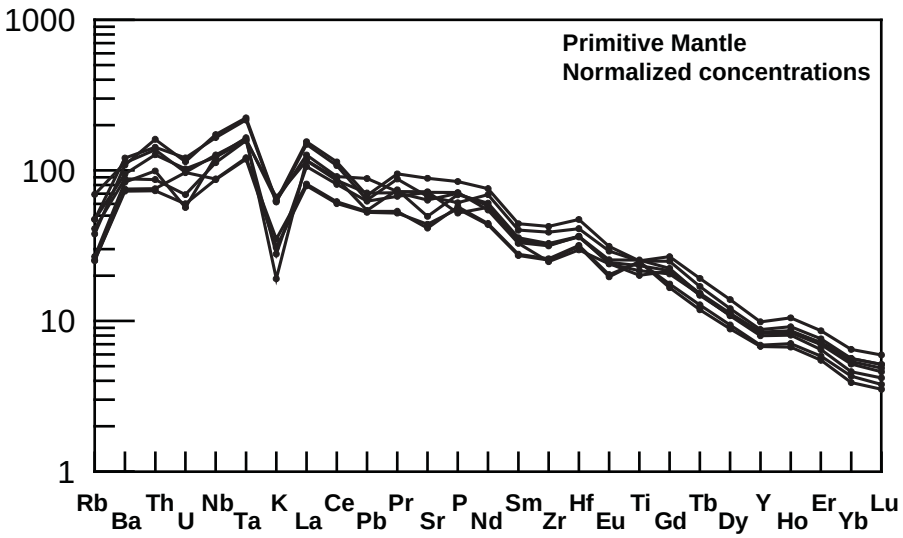
1000
100
10
1
Primitive Mantle
Normalized concentrations
Rb
Ba
Th
U
Nb
Ta
K
La
Ce
Pb
Pr
Sr
P
Nd
Sm
Zr
Hf
Eu
Ti
Gd
Tb
Dy
Y
Ho
Er
Yb
Lu

Figure DR6

Table DR1.

Sample	Latitude ^{o}N	Longitude ^{o}E
3183	9.76733	38.4668
3184	9.76958	38.4948
3185	9.79287	38.5389
3186	9.81111	38.5514
3187M	9.79482	38.6809
3187T	9.79482	38.6809
3188M	9.78819	38.6891
3188T	9.78819	38.6891

T**able DR2**. XRF data on major and selected trace elements for the Gerba Guracha lavas and replicate measurements. Given standard values are colored in green.

Sample	Date	SiO2 (%)	TiO2 (%)	Al2O3 (%)	Fe2O3 (%)	MnO (%)	MgO (%)	CaO (%)	Na2O (%)	K2O (%)	P2O5 (%)	Totals (%)	LOI (%)	Ni (PPM)	Rb (PPM)	Sr (PPM)	Zr (PPM)
3183	4/17/10	37.72	4.46	11.36	15.58	0.23	6.25	14.88	2.68	0.8	1.48	95.44	4.21	<40	26	1508	277
3183	5/24/10	37.56	4.41	11.32	15.56	0.23	6.25	14.83	2.66	0.8	1.47	95.09	4.59	<40	27	1505	277
3184	4/17/10	38.34	5.18	12.37	13.59	0.23	5.63	13.67	2.75	1.8	1.75	95.31	4.3	<40	24	1869	475
3184	5/24/10	38.2	5.17	12.33	13.58	0.23	5.65	13.65	2.75	1.8	1.76	95.12	4.5	<40	23	1867	475
3185	4/17/10	38.01	5.13	10.71	15.64	0.19	7.31	14.48	2.4	1.01	1.2	96.08	3.7	<40	16	874	290
3185	5/24/10	37.74	5.13	10.66	15.58	0.19	7.31	14.44	2.41	1.01	1.2	95.67	4.1	<40	16	870	289
3186	4/17/10	37.85	5.16	10.6	15.81	0.19	7.26	15.17	2	0.89	1.16	96.09	3.68	<40	16	925	284
3186	5/24/10	37.73	5.2	10.55	15.79	0.19	7.25	15.13	1.98	0.88	1.16	95.86	3.9	<40	17	925	284
3187M	4/17/10	39.34	5.19	12.84	13.17	0.21	5.27	13.27	3.4	1.78	1.27	95.74	3.91	<40	30	1419	435
3187M	5/24/10	39.21	5.16	12.82	13.18	0.21	5.27	13.26	3.43	1.78	1.25	95.57	4.1	<40	30	1417	435
3187T	4/17/10	37.56	5.28	10.92	14.97	0.2	7.75	14.53	2.7	0.55	1.44	95.9	3.82	<40	17	1044	366
3187T	5/24/10	37.47	5.31	10.88	14.98	0.2	7.72	14.52	2.7	0.55	1.43	95.76	3.98	<40	17	1043	365
3188M	4/17/10	39.66	4.84	11.45	13.91	0.2	6.16	14.22	2.08	1.92	1.47	95.91	3.77	<40	30	1339	358
3188M	5/24/10	39.44	4.78	11.4	13.87	0.2	6.12	14.17	2.08	1.92	1.47	95.45	4.24	<40	31	1337	356
3188T	4/17/10	42.87	4.15	13.39	12.31	0.19	5.17	10.94	3.42	1.81	1.08	95.33	4.32	<40	44	1519	353
3188T	5/24/10	42.68	4.14	13.34	12.31	0.19	5.19	10.92	3.43	1.82	1.07	95.09	4.58	<40	45	1519	353
BHVO-1	4/17/10	49.42	2.72	13.42	12.1	0.17	7.17	11.36	2.21	0.52	0.28	99.37	0.49	113	7	386	175
BHVO-1	5/24/10	49.24	2.71	13.36	12.1	0.17	7.16	11.34	2.21	0.52	0.28	99.09	0.78	113	8	386	174
BHVO-1		49.94	2.71	13.80	12.23	0.17	7.23	11.40	2.26	0.52	0.27	100.53		121	9.5	390	180
JA-3	5/24/10	61.83	0.68	15.64	6.54	0.1	3.8	6.23	3.09	1.39	0.11	99.41	0.48	<40	35	280	117
JA-3		62.26	0.68	15.57	6.59	0.106	3.65	6.28	3.17	1.41	0.11	99.826		36	36	294	119
W-2	4/17/10	52.66	1.07	15.31	10.76	0.17	6.44	10.93	2.18	0.63	0.13	100.28	0	78	18	192	101
W-2		52.44	1.06	15.35	10.74	0.16	6.37	10.87	2.14	0.63	0.131	99.891		74	20	192	92

T**able DR3.** LA-ICPMS Trace element data for the Gerba Guracha lavas. Values for the standard Jb1a, Jb2, Jb3, and W2 run as unknowns throughout the day is also shown.

sample	Ba	La	Ce	Pr	Nd	Sm	Eu	Gd	Tb	Y	Dy	Ho	Er	Yb	Lu	V	Cr	Nb	Hf	Ta	Pb	Th	U
3183	614	72.9	143.4	18.57	73.9	14.5	4.02	12.2	1.62	37.8	8.11	1.37	3.34	2.55	0.34	301	2.76	80.2	9.16	6.47	4.44	7.39	1.45
3184	758	106.5	202.0	26.14	102.5	19.6	5.25	15.9	2.07	44.9	10.22	1.72	4.13	3.19	0.44	242	2.13	123.4	14.59	9.15	4.84	13.68	2.4
3185	525	55.7	110.0	14.75	60.2	12.3	3.41	10.5	1.38	31.4	6.93	1.16	2.8	2.12	0.28	304	15.03	62.5	9.81	4.97	3.79	6.42	2.03
3186	509	54.3	106.9	14.36	59.1	12.1	3.3	9.9	1.28	30.8	6.52	1.1	2.63	1.92	0.26	303	14.2	62.0	9.66	4.87	3.74	6.23	1.26
3187M	844	102.3	191.4	24.21	93.5	17.8	4.89	14.9	1.83	39.9	8.9	1.5	3.65	2.78	0.38	270	2.59	117.8	12.67	8.86	4.51	12.11	2.54
3187T	584	80.2	156.9	20.5	82.1	15.9	4.28	13.3	1.62	36.3	7.98	1.32	3.1	2.27	0.31	283	44.49	87.7	11.26	6.75	3.85	8.42	1.19
3188M	660	79.6	152.5	19.6	78.7	15.2	4.11	12.8	1.65	38.4	8.29	1.41	3.44	2.65	0.36	276	13.34	87.4	11.17	6.5	5.02	10.8	2.15
3188T	784	86.9	161.5	19.94	77.0	14.7	4.04	12.8	1.6	37.9	8.06	1.39	3.44	2.78	0.38	233	21.85	90.3	11.28	6.6	6.27	11.65	2.04
jb1a	489	36.3	65.1	7.04	26.2	5.1	1.48	4.9	0.72	24.0	4.12	0.79	2.17	2.12	0.3	209	383.6	28.5	3.41	1.82	6.1	9.05	1.61
jb1a	504	37.0	66.9	7.15	26.7	5.1	1.48	5.0	0.7	23.6	3.99	0.77	2.15	2.06	0.3	211	389.6	28.3	3.41	1.81	6.18	9.18	1.66
jb1a	496	37.1	67.8	7.18	26.9	5.1	1.52	4.9	0.72	23.4	4.04	0.78	2.17	2.14	0.3	215	401.3	28.9	3.56	1.87	6.34	9.63	1.76
jb2	206	2.4	6.3	1.07	6.5	2.3	0.85	2.9	0.59	26.9	4.11	0.89	2.68	2.76	0.41	513	29.33	0.6	1.6	0.05	5.18	0.26	0.13
jb3	226	8.5	21.1	3.25	15.9	4.2	1.3	4.3	0.74	27.9	4.66	0.94	2.69	2.67	0.39	371	60.82	2.2	2.9	0.16	5.47	1.35	0.45
w2	171	10.6	23.5	3.01	13.2	3.4	1.11	3.5	0.62	23.0	3.84	0.78	2.29	2.18	0.31	266	81.44	7.7	2.57	0.5	6.17	2.31	0.49

Table DR4. Sr isotope measurements were performed on a multicollector Finnigan MAT26X mass spectrometer upgraded by Spectromat. Instrumental mass fractionation was corrected using $^{86}Sr/^{88}Sr$ =0.1194. Repeat analyses of NBS 987 during the analysis period gave an average value of 0.71025 ± 3 (2σ, n=5). All Hf, Pb and Nd isotope measurements were made on a Thermo Neptune multi-collector inductively coupled plasma mass spectrometer at IFREMER. Repeat measurements of the Hf isotope standard JMC 475 during the course of the analyses yielded reproducibility of 13ppm (2σ, n=13) on $^{176}Hf/^{177}Hf$ with a value of 0.282165. The Pb isotope data are reported relative to published values for NBS 981 in Catanzaro et al., (1968). The samples were spiked with thallium to correct for mass fractionation. Repeat measurements of rock standard JB-2 during the course of the analyses yielded $^{206}Pb/^{204}Pb$ = 18.338±4, $^{207}Pb/^{204}Pb$= 15.553±3, $^{208}Pb/^{204}Pb$ = 38.271±10 (2σ, n=4). Repeat measurements of the Nd isotope standard JNdi-1 (Tanaka et al., 2000) yielded $^{143}Nd/^{144}Nd$ values of 0.512116 ± 7 (2σ, n=12).

Sample	$^{87}Sr/^{86}Sr$	2σ	$^{143}Nd/^{144}Nd$	2σ	$^{206}Pb/^{204}Pb$	2σ	$^{207}Pb/^{204}Pb$	2σ	$^{208}Pb/^{204}Pb$	2σ	$^{176}Hf/^{177}Hf$	2σ
3183	0.703994	7	0.512764	4	20.024	0.001	15.779	0.001	40.216	0.004	0.282822	8
3184	0.703741	10	0.512743	4	19.789	0.001	15.734	0.001	40.027	0.003	0.282794	8
3185	0.703858	7	0.512741	6	19.658	0.002	15.735	0.002	39.892	0.005	0.282795	9
3186	0.703844	7	0.512733	5	19.613	0.001	15.731	0.001	39.897	0.003	0.282799	9
3187M	0.703712	8	0.512752	5	19.618	0.001	15.715	0.001	39.824	0.004	0.282800	9
3187T	0.703690	7	0.512759	5	19.879	0.001	15.744	0.001	40.064	0.003	0.282802	9
3188M	0.704063	9	0.512725	5	19.314	0.001	15.696	0.001	39.643	0.004	0.282797	10